Origin of abnormally sharp features in collision-induced spectra of cryosolutions

Reference:

Herrebout Wouter, van der Veken Benjamin, Kouzov A.P., Filippov N.N..- Origin of abnormally sharp features in collision-induced spectra of cryosolutions

The journal of chemical physics - ISSN 0021-9606 - (2015), p. 1-24

Origin of Abnormally Sharp Features in Collision-Induced Spectra of Cryosolutions

W.A. Herrebout,[1, a)] B.J. van der Veken,[1] A.P. Kouzov,[2, b)] and N.N.Filippov[2]

[1)] *Department of Chemistry, University of Antwerpen, Groenenborgerlaan 171, 2020 Antwerpen, Belgium*

[2)] *Department of Physics, Saint Petersburg State University, Peterhof, Ulianovskaya str. 3, Saint Petersburg 198504, Russia*

A weak, paradoxically narrow resonance feature (shortly, the r-line) near the O_2 fundamental frequency in the collision-induced absorption spectrum of oxygen dissolved in liquid argon and liquid nitrogen (T=89 K) is resolved for the first time. An accurate band shape fitting routine to separate the r-line from the by-far more intense diffuse background and to study its behavior versus the oxygen mole fraction x which ranged from 0.03 up to 0.23 has been elaborated. At small $x(\lesssim 0.07)$, the r-line intensity was found to scale as x^2 leaving no doubt that it is due to the solute-solute (O_2-O_2) interactions. In line with our results on the pH_2-LNe cryosystem (W.A. Herrebout et al, Phys. Rev. Lett. **101**, 093001 (2008)), the Lorentzian r-line shape and its extraordinary sharpness (HWHH$\approx$ 1 cm^{-1}) are indicative of the motional narrowing of the relative solute-solute translational spectrum. As x is further raised, ternary solute-solute interactions impede the r-line growth in the O_2-LAr spectrum because of the cancellation effect (J. van Kranendonk, Physica **23**, 825 (1957)). Theoretical arguments are given that multiple interactions between the solutes should finally destroy the solute-solute induced r-line when the mixed solution approaches the limit of the pure liquid ($x = 1$). Interestingly, the nonbinary effects are too weak to appreciably affect the quadratic r-line scaling in the O_2-LN_2 cryosystem which persists up to x=0.23. It is emphasized that studies of the resonant features in the collision-induced spectra of binary cryosolutions open up unique opportunities to spectroscopically trace the microscopic-scale diffusion.

[a)] Electronic mail: Wouter.Herrebout@ua.ac.be

[b)] Electronic mail: alex@ak1197.spb.edu

I. INTRODUCTION

Couplings between the electromagnetic field and the dipole moments of isolated molecules give rise to conventional, or allowed absorption spectra from which a richly featured picture of the intramolecular motion can be restored. However, the information on the molecular translational dynamics obtained therewith is rather limited and indirect. The situation was greatly improved upon the discovery[1] of collision-induced absorption (CIA) whose origin owes to incremental dipole moments induced by the intermolecular interactions. Evidently, these dipole moments are strongly modulated by molecular translations which become the key factor in the formation of CIA spectra. In turn, CIA offers outstanding possibilities to trace the intermolecular dynamics in all phases,[2–5] by far exceeding those of the allowed-absorption spectroscopy.

Since the lifetimes of the collision-induced moments are of the order of one picosecond, the CIA bands in gases and liquids are diffuse, with the widths ranging from tens to hundreds of cm^{-1}. The sole exception is provided by richly featured bound-state transitions in the van-der-Waals complexes observable at relatively low pressures and temperatures; however, their line structure quickly coalesces at densities of ten Amagats or higher at which most of the CIA measurements are performed. Based on these facts, it was commonly believed that the CIA bands in fluids and liquids should be diffuse just because the translational motion in such systems is rapid and chaotic. From this point of view, the appearance of the sharp quasi-Lorentzian line (hereafter, the r-line) at the center of the diffuse CIA fundamental band of nitrogen dissolved in liquified noble gases (Ar, Kr, Xe, or shortly, Rg)[6] is paradoxical. Its half width at half height (HWHH) Γ_r for the N_2-LAr (T=83 K) system was less than 1 cm^{-1}, in striking contrast with the background spectrum whose HWHH was about 60 cm^{-1}. It is also worth noting that the r-line develops quite close, with a mere blue shift of 0.5 cm^{-1}, to the fundamental vibrational frequency $\tilde{\nu}_0$ of N_2 in the liquid phase[7] ($\tilde{\nu}_0$=2326.6 cm^{-1}) and is thus reliably assigned to this mode.

The striking sharpness of the r-line[6] implies that an anomalously long-living polarization is formed in the studied cryosystems, a feature which, to our knowledge, had never been reported for the CIA spectra of dense systems with chaotic translational motion. The studies[6] of the $r-$line integrated intensity $M_r^{(0)}$ as a function of the mole fractions of N_2 (x_A) and Rg (x_B) revealed correlation between $M_r^{(0)}$ and $x_A x_B$. Based on this result, the

anomalous feature was ascribed[6] to stable N_2-Rg complexes.

However, several points remain unclear or questionable in that theory. First, it was unclear why an Rg atom surrounded by N_2 molecules or, *vice versa*, an N_2 molecule in the bulk of a liquified noble gas interacts so strongly only with a single solvent particle and remains uncoupled to others? Besides, the N_2-N_2 and N_2-Rg potentials are rather similar and one may also ask why no resonant features are seen in the CIA spectrum of pure liquified nitrogen in which the dimerization should also occur? Notice also that the advanced complexation picture implies the existence of a local potential well in the nearest surrounding. The studies[6] of the $M_r^{(0)}$ vs T behavior gave the complexation energy $E_0(N_2\text{-Ar})/hc$ =125 cm^{-1}. Since E_0 is only twice the mean kinetic energy (kT) and because of the high rate of interactions with the surrounding, the complexes should be rather unstable so that the N_2-Rg (quasi)bond is expected to quickly switch to another neighbouring Rg atom. Such instability should certainly show up in a substantial broadening incompatible with the experimental observation.

Conventionally, the terms of the collision-induced dipole moments are referred to as isotropic - which are independent on the rotational degrees of freedom - and anisotropic ones, entirely modulated by the molecular rotation. For relatively light rotators like N_2, this modulation creates additional broadening which can reach about 30 cm^{-1} at 90 K and, owing to it, diffuse unresolved translation-rotation bands appear in the spectra of gas[1,8,9] and liquid[6,10] phases. Therefore, the origin of the $r-$line is completely due to the isotropic part of the collision-induced dipole moment.

A qualitative analysis of the spectrum of the bound-bound translational transitions based on the widely used spherically symmetric square-well potential model[11,12] can also serve as a touchstone for the complexation hypothesis. Emergence of the discrete eigenstates for this potential is determined by the dimensionless parameter $\varepsilon = 2m_c U_0 r_c^2/\hbar^2$ where m_c is the reduced mass of the complex and r_c is the radius of the well. The radius value can be estimated by using the cage model of liquid[13,14] that gives in the N_2-Ar case $r_c \approx 1 a.u.$ whereas E_0 can serve as a quick estimation of the potential well depth U_0. Using $U_0(N_2\text{-Ar})/\text{hc} \approx E_0/hc$ =125 cm^{-1}, one obtains $\varepsilon \approx 25$ which results in three bound ns states $n = 1, 2, 3$[11] and a few higher lying $np, nd, ...-$ levels. In doing so, the total number of the bound states is estimated to be close to ten, with an average splitting between adjacent levels of the order of 10 cm^{-1}. Since the isotropic induced dipole moment varies as the first-

rank spherical harmonics of the N_2-Rg bond orientation in space, the selection rule $\Delta l = \pm 1$ for the angular momentum quantum numbers l holds and, hence, pairs of the satellite lines shifted by about ten cm^{-1} from $\tilde{\nu}_0$ should appear. In this scenario, the appearance of a singlet $r-$line is imaginable only when the relative N_2-Rg translations are totally frozen which does not hold at temperatures used either presently or in Ref.[6]. In a more realistic picture, all bound states, especially the upper ones, are strongly broadened because a weak complex is easily destroyed by neighboring particles. As the result, the complexation should rather manifest itself in a diffuse unresolved doublet whose width by far exceeds that of the observed resonance line.

In view of these doubts, the $r-$line problem should be revisited, also because of the complexation hypothesis conflicts with the results of recent IR studies[15,16] of *para*-hydrogen solutions in liquid Ne ($0.0023 \leq x_{H_2} \leq 0.036$) where a similar, anomalously sharp line developing at the fundamental vibrational frequency of H_2 was detected. Accurate band shape fittings[16] showed the line to consist of two components, the sharper $r-$component ($\Gamma_r \approx 1.7$ cm^{-1}) whose intensity scaled exactly as $x_{H_2}^2$ and a several times more diffuse one. The latter component, developing linearly with x_{H_2}, was attributed to the interaction of a guest with a local defect (vacancy). The intensities of both components compete at very high dilutions, but as x_{H_2} reaches ≈ 0.03 the diffuse feature becomes poorly seen under the by far more intense $r-$line. These conclusions are in conflict with the N_2-Rg complexation theory based on the $M_r^{(0)} \sim x_A$ proportionality at high dilutions ($x_A \ll 1, x_B \approx 1$). Moreover, the N_2-LAr system was scrutinized at $x_A \geq 0.1$ which in view of the studies[15,16] do not seem to be sufficiently low and, therefore, the measurements should be extended to higher dilutions. Besides, as found in Refs.[15,16], the results of the $r-$line separation strongly depend on the accuracy of the background fittings. Hence, the Gaussian profiles used in Ref.[6] to mimic the background intensity distributions lack flexibility, and more robust fittings are therefore desirable.

Here, the yet unstudied collision-induced fundamental oxygen absorption spectra of the O_2-Ar and O_2-N_2 cryosolutions at T=89 K are reported. As in the case of the nitrogen cryosolutions,[6] a distinct $r-$feature was detected and its transformation with x_{O_2} was traced from 0.23 down to 0.03 , i.e. at higher dilutions than were used for the N_2-LAr system.[6] Besides, finer variations of x_{O_2} produced a detailed picture of the $r-$line transformations in the concentration range crucial to comprehend the origin of this intriguing feature.

II. EXPERIMENTAL DETAILS

The absorbances were recorded in an optical cell of 1 cm pathlength by using a Bruker IFS 66v interferometer at 0.5 cm^{-1} resolution, in combination with a Si/CaF_2 beamsplitter, a tungsten source, and an InSb detector, by averaging 1000 scans and applying Blackmann-Harris apodization. Temperature was fixed at 89 K. The working pressure in the cell was about 20 bars for both cryosystems. Argon, nitrogen and oxygen obtained from Air Liquide had a stated purity of 99.9999% and were used without further purification. The estimated mole fraction uncertainty was of the order of 0.001 to 0.015 that gives, in the mean, the relative uncertainty $\delta x_{O_2}/x_{O_2} \approx 5\%$.

III. RESULTS AND DISCUSSION

A. Spectral fittings

The recorded bands consist of diffuse, structureless pedestals on which the weak $r-$lines develop at ≈1551.4 cm^{-1} (in LAr) and ≈1552.5 cm^{-1} (in LN_2) (Fig. 1), in a close proximity to the fundamental band origin of a free O_2 molecule (1555.7 cm^{-1} (Refs.[17,18])) or even closer to the values obtained for pure LO_2 (1551.7[19]; 1552.7[20]). As in the previously studied cases,[6,15,16] the $r-$line is easily identified as belonging to the fundamental vibrational transition.

Except in the frequency range near the $r-$line, the concentration growth, especially for the solutions in nitrogen, does not drastically change the absorption shapes (see Figs. 2 and 3). Generally, as $x(= x_{O_2})$ is increased, the spectra of both cryosolutions are slightly narrowed and tend to shift to lower frequencies. For illustrative purposes, the relative absorbances (i.e. ones normalized by unity at $\tilde{\nu} = 1560$ cm^{-1} where the background intensities reach their maxima) are drawn on these figures.

The $r-$lines vs x behavior is the most striking feature of the studied spectra. As evident from the insets to Figs. 2 and 3, the $r-$lines increasingly manifest themselves against the normalized background implying these lines to scale much faster than x. More definite conclusions can be drawn only on the basis of refined shape fittings that should be desirably done with an accuracy approaching the noise track of the recorded spectra.

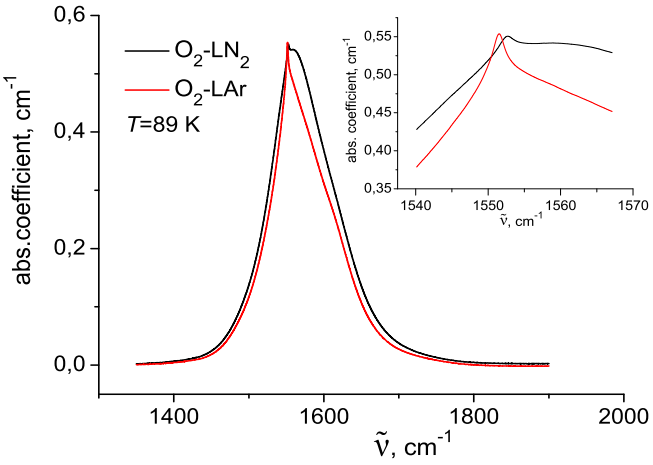

FIG. 1. Fundamental oxygen absorption in the oxygen-nitrogen (black line) and oxygen-argon (red line) cryosolutions at the oxygen mole fraction x=0.088. Inset shows enlarged parts of the spectra around the resonance line at 1552 cm^{-1}.

The central part of the background was simulated by using the function[16,21]

$$S_d(\Delta\omega_d) = Q(\hbar\Delta\omega_d/kT)S_d(0)\exp[\gamma - \sqrt{\gamma^2 + (\Delta\omega_d/\omega_c)^2}] \qquad (1)$$

with three varied parameters, $S_d(0), \omega_c$ and the band origin ω_d; $\Delta\omega_d = \omega - \omega_d$. The background shape asymmetry evident from Figs. 1-3 was accounted for by the quantum Boltzmann factor Q. Generally, the asymmetry is a quantum statistical effect which affects the spectral distribution $S(\Delta\omega_m)$ around the self frequency ω_m of a certain mode. In particular, the equation $S(-\Delta\omega_m) = exp(-\hbar\Delta\omega_m/kT)S(\Delta\omega_m)$ holds whenever the mode-bath couplings are weak; besides, its validity is favored by relatively small detunings $\Delta\omega_m = \omega - \omega_m$ used in our analysis. Under these conditions, the use of the conventional factor[3] $Q(x) = 2/[1+\exp(-\hbar x/kT)]$ to mimic the background asymmetry as well as that of the $r-$ and $v-$ lines (see below) is justified.

It is also worth noting that the quantum asymmetry can considerably shift the shape maximum from ω_m to higher frequencies. The effect is increased as the shape half width becomes comparable to kT/hc . For both cryosystems studied, the background HWHHs are close to kT/hc(=61.9 cm^{-1}) so that the shifts of the background maxima from ω_d are quite sizeable (∼7 cm^{-1}, see Fig. 4).

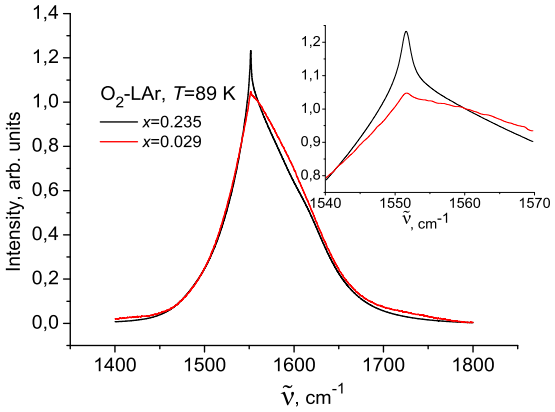

FIG. 2. Transformation of the O_2-LAr absorption band shape with x. Intensities are normalized by unity at $\tilde{\nu} = 1560$ cm^{-1}. Spectral range around the $r-$line is shown on the inset.

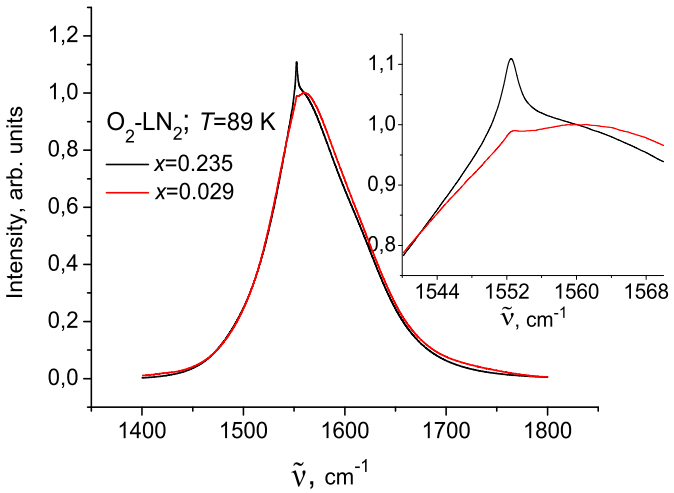

FIG. 3. Transformation of the O_2-LN_2 absorption band shape with x. Intensities are normalized by unity at $\tilde{\nu} = 1560$ cm^{-1}. Spectral range around the $r-$line is shown on the inset.

As it follows from Eq. (1), variations of the fourth parameter, γ, affect the shape mainly near the origin; namely, as γ tends to zero, the shape near the maximum becomes sharper. As seen from Fig. 1, the background shapes in LAr are sharper and more narrow than those

in LN_2. The most likely reason is that the O_2-N_2 induced dipole moment is also affected by the N_2 rotation which provides an additional broadening channel compared to the O_2-Ar case. In compliance with these arguments, preliminary spectral fits for diluted solutions showed that the optimal values of γ to be close to 0.25 (LAr) and 0.5 (LN_2). To avoid overparametrization, these values were further fixed for the remaining spectral fittings.

At the first stage, we tried to mimic the observed shapes by a linear combination of $S_d(\Delta\omega_d)$ and a resonance lorentzian line, $L_r(\Delta\omega_r)$, centered at ω_r. For consistency, this line was also corrected for the detailed balance by the same $Q(\Delta\omega_r)$ factor. The fittings were performed in the 1540-1570 cm^{-1} interval encompassing the resonance line by using the ORIGIN 7.5 software package. As in the previously studied $p\mathrm{H_2}-$LNe case,[15,16] it was calculated that such division of the total shape into two components with drastically different widths is insufficient to reproduce the observed spectral distributions within the experimental uncertainty. Actually, regular deviations were observed at detunings several times larger than the Lorentzian HWHH Γ_r. This disbalance was perfectly cancelled by introducing another asymmetric Lorentzian $L_v(\Delta\omega_v)$ several times broader than $L_r(\Delta\omega_r)$. Its inclusion is in compliance with our analysis[15,16] of the $p\mathrm{H_2}-$LNe cryosystem ($x_{H_2} \leq 0.036$) where the broader component (hereafter referred to as the $v-$line) was attributed to the interaction of a solute with a defect (vacancy) formed in the first coordination sphere. Since the rotational broadening much exceeds the calculated half widths of the $v-$line, this feature, much like the r-line, was associated with the isotropic polarization. In contrast to the previous fittings,[15,16] the $v-$line origin ω_v was found to be sizeably different from ω_r; however, the difference can be assigned to the effect of the much higher solute concentrations used in the present study. As exemplified by Fig. 4, the optimized profiles are very nearly indistinguishable from the experimental curves, allowing to reliably trace the concentration behavior of the $r-$ and $v-$lines.

B. Concentration dependencies

In diluted solutions ($x \ll 1$), the integrated background absorption coefficients (zero-order moments) $M_b^{(0)}$ scale linearly with x, corresponding to the regime when the solutes are isolated in the bulk of solvent molecules and the effect of the O_2-O_2 interactions on $M_b^{(0)}$ is negligible. Since each solute is typically surrounded by 10-12 neighbors, one can

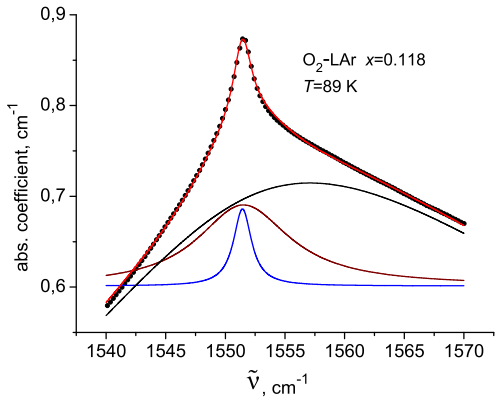

FIG. 4. Example of experimental spectrum (dots) separation into the $r-$ (blue curve), $v-$ (brown curve) and the background (black curve) contributions. The $r-$ and $v-$ lines are shifted upward by 0.6 cm^{-1}. The red line denotes the simulated total profile.

expect that at $x \gtrsim 0.1$ the linear scaling will be increasingly distorted by the binary, ternary, ... etc. solute-solute interactions. To study these effects, the experimentally accessible total band moments $M^{(0)}$ can be used instead of $M_b^{(0)}$ without noticeable loss of accuracies, for the $r-$ and $v-$lines contribute to $M^{(0)}$ quite negligibly (by 2% or less). We found that in the studied $x \leq 0.235$ range, the sets of $M_k^{(0)}$ (where k =1,2,...N numbers a particular measurement and $N = 10$ is the total number of measurements for each cryosystem) can be accurately fitted by the parabolic functions:[22] $M^{(0)}/\mathrm{cm}^{-2}$=570(30)x +510(140)x^2 (LAr) and $M^{(0)}/\mathrm{cm}^{-2}$= 590(80)x +1800(460)x^2 (LN_2) whose quadratic coefficients characterize the O_2-O_2 interactions in the solvent surrounding. Thus, the absorption induction for both infinitely diluted solutions is very similar but the binary coefficients differ quite strong.

We further notice that the experimental $M^{(0)}$ values have accuracies better than one per cent, implying their scattering from smooth dependencies to be caused by inaccuracy of the concentration measurements. The derived parabolic functions were used to find the corrected values x_k from the equation $M_k^{(0)} = M^{(0)}(x_k)$ which are less liable to errors than the direct concentration measurements. The thus corrected sets x_k were used as the input mole fractions to analyze the behavior of the sharper components.

We first discuss the key characteristics of the $r-$ line. Its moments, $M_r^{(0)}$, are presented on Fig. 5 for both cryosystems. At $x \lesssim 0.1$, both dependencies scale as x^2, i.e. in the same

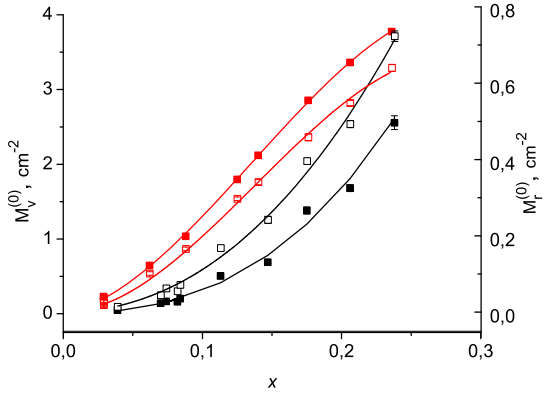

FIG. 5. Zeroth-order moments of the $r-$ (empty squares) and $v-$ (filled squares) lines as functions of oxygen mole fraction for O_2-N_2 (black) and O_2-Ar (red) cryosolutions. The $M_r^{(0)}$ data refer to the right hand scale. Least-squares fits are denoted by solid lines.

fashion as the similar characteristics of the diluted $p-H_2$-LNe cryosolution. This suggests that in this concentration range the $r-$lines are induced by the binary self-interactions, in line with previous work.[15,16] To emphasize the different concentration scaling of the $M_r^{(0)}$ and $M^{(0)}$ moments, we plot on Fig. 6 their ratio as a function of x. Since the total band moment $M^{(0)}$ in dilute solutions scales as x, the observed linear dependence of the moment ratio on x (Fig. 6) is an indication of the proportionality between $M_r^{(0)}$ and x^2.

As the oxygen content grows, the ternary effects varying as x^3 increasingly show up. The least-squares fittings show that the two-term power expansion for the O_2-LAr cryosystem $M_r^{(0)}/\mathrm{cm}^{-2}$ =26.3(7)x^2-65(5)x^3 adequately represents the measurements. In the O_2-LN_2 case, the same dependence is nearly quadratic ($M_r^{(0)}/\mathrm{cm}^{-2}$ ≈12.2(7)x^2) so that the cubic coefficient can not be reliably determined. Thus, the effect of ternary collisions on the $r-$line induction is stronger in the LAr solution.

The half widths, Γ_r, also demonstrate regular (linear) decrease with x: (O_2-LAr) $\Gamma_r/\mathrm{cm}^{-1}$=1.14(1)-1.2(1)$x$; ($O_2-LN_2$) $\Gamma_r/\mathrm{cm}^{-1}$=1.28(3)-0.9(3)$x$. Figure 7 shows that the positions $\tilde{\nu}_r(=\omega_r/2\pi c)$ of the $r-$line maxima linearly drift with x in the opposite directions : (O_2-LAr) $\tilde{\nu}_r/\mathrm{cm}^{-1}$=1551.37(1)+0.7(1)$x$; ($O_2-LN_2$) $\tilde{\nu}_r/\mathrm{cm}^{-1}$=1552.54(1)-0.45(5)$x$. Again, different concentration behavior of the $v-$lines was found for both solvents. Although these lines are red-shifted with x (Fig. 7), the effect is more pronounced for the solutions in argon:

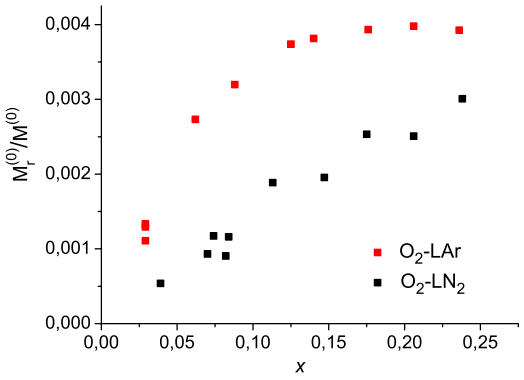

FIG. 6. Dependence of the ratio of the r-line integrated intensity to the total band intensity on oxygen mole fraction x.

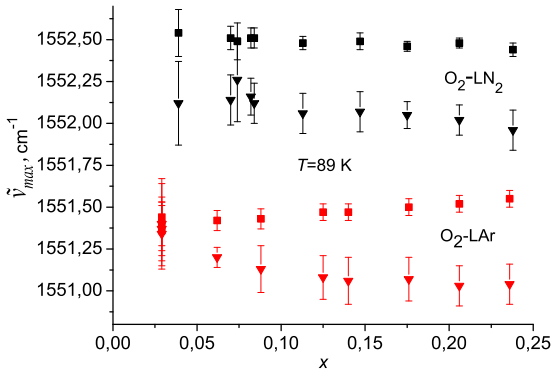

FIG. 7. Dependence of the $r-$ (squares) and $v-$ (triangles) line maxima on oxygen mole fraction x for solutions in liquid nitrogen (black) and liquid argon (red).

$\tilde{\nu}_v$=1551.36(4)-1.7(3)x (O_2-LAr) ; $\tilde{\nu}_v$=1552.18(2)-0.8(2)x (O_2-LN_2).

The $M_v^{(0)}$ vs x behavior is definitely nonlinear and requires polynomial fittings. However, because of the low statistical weight of measurements in highly diluted solutions, such fittings produce unreliable linear coefficients. The slopes $dM_v^{(0)}(x)/dx$ at x=0 were estimated by the ratio $M_v^{(0)}(x)/x$ for the lowest concentration (x=0.029) and were further kept constant. After the inclusion of the quadratic and cubic terms, fits accurately reproduced the measured moments (Fig. 5). In the O_2-LAr case we derived: $M_v^{(0)}/\mathrm{cm}^{-2}$=7$x$+85(5)$x^2$ -190(25)x^3;

the quadratric term for the O_2-LN_2 solution was found to be statistically insignificant and the optimal fit was $M_v^{(0)}/cm^{-2}=1.2x+175(7)x^3$. Therefore, the $M_v^{(0)}$ moments (Fig. 5) reveal different behavior of the $v-$line in the studied cryosystems. Very weak, but opposite tendencies are observable in the Γ_v vs x behavior: in the O_2-LAr solution the $v-$line is slightly narrowed with increasing x, whereas in the O_2-LN_2 case a feeble broadening seemingly holds. Unfortunately, the data scattering and the weakness of the effect plague a reliable $\Gamma_v(x)-$slope determination; because of this, only the mean values are cited herewith: (O_2-LAr) $\Gamma_v=5.94(4)cm^{-1}$ and (O_2-LN_2) $\Gamma_v=4.9(2)cm^{-1}$. Taken altogether, the aforemetioned results are evidence that the concentration differently changes the microdynamics of the O_2 solutes in both cryosystems.

The concentration also affects the background shape parameters. For both cryosolutions, the origins are shifted to lower frequencies as x is raised: (O_2-LN_2) $\tilde{\nu}_d/cm^{-1}=1553.7(2)-2(1)x$ and (O_2-LAr) $\tilde{\nu}_d/cm^{-1}=1552.91(3)-1.9(3)x$. Remarkably, in the infinitely diluted solutions, the origins of the background and of the $r-$line differ measurably, cf. $\tilde{\nu}_d(x=0)/cm^{-1}=1552.91(3)$ and $\tilde{\nu}_r(0)/cm^{-1}=1551.37(1)$ (LAr); $\tilde{\nu}_d(0)/cm^{-1}=1553.7(2)$ and $\tilde{\nu}_r(0)/cm^{-1}=1552.54(1)(LN_2)$. This is expectable since $\tilde{\nu}_r(0)$ is always affected by the presence of another O_2 neighbour which shifts the vibrational frequency whereas $\tilde{\nu}_d(0)$ is solely determined by the action of the solvent. Besides, the $\tilde{\nu}_c$ parameter (Eq. 1) which correlates with the width of the central part of the background was found to regularly decrease with x: (O_2-LN_2) $\tilde{\nu}_c/cm^{-1}=43.9(2)-13(2)x$ and (O_2-LAr) $\tilde{\nu}_c/cm^{-1}=51.4(3)-16(2)x$ which manifests itself in slight concentration narrowing of the band shapes (see Figs. 2 and 3).

C. Discussion

1. General remarks

To interpret the observed effects, the theoretical approach[15,16] should be extended to incorporate the ternary interactions as the present concentrations are substantially higher than those used previously.[15,16] Also, account should be taken of the fact that the rotation of the O_2 molecule, in contrast to that of H_2, is strongly perturbed by its surrounding. As a result, the rotational structure on Figs. 1-3 disappears but the hindered rotation still substantially contributes to the band widths.

To perceive the origin of different CIA features, the behavior of the net polarization $\mathbf{M}$ vibrating at the solute frequency ω_0 must be examined. For that, we use the conventional pairwise induction scheme

$$\mathbf{M} = \sum_{ab} \mathbf{m}_{ab} + \sum_{c\alpha} \mathbf{d}_{c\alpha} \tag{2}$$

where $\mathbf{d}_{c\alpha}$ and $\mathbf{m}_{ab}$ are the dipole moments induced by the binary guest-host $(c-\alpha)$ and guest-guest $(a-b)$ interactions, correspondingly. The summations are performed over the N host and the N_1 guest particles, which are hereafter designated by Greek and Latin letters, respectively.

Our approach is similar to that developed by Van Kranendonk[23] for moderately compressed gases for which the CIA integrated intensity is rigoriously expanded in powers of the number density ρ. However, in our case the polarization dynamics is intrinsically complicated by many-body interactions with solvent particles. In a dilute solution, the collective, many-body terms (A) can be separated from $\mathbf{M}$ which depend on the position of a spectroscopically active solute (a) relative to the surrounding solvent molecules. These terms are responsible for the diffuse spectrum induction provided there are no long-living defects (vacancies) in the vicinity of a. Second, the terms B which depend on the distance $\mathbf{R}$ between a and some other selected (quasi)particle can arise when two solutes meet in the bulk of solvent or when a solute interacts with a vacancy in the first coordination sphere.[15,16] The B-type signatures appear as sharp, near-Lorentzians peaks easily distinguished from a diffuse background produced by the collective A-terms.

At extremely high dilutions, the time autocorrelation function (TACF) $C(t)$ of $\mathbf{M}$ reads

$$C(t) \equiv \langle(\mathbf{M}(0), \mathbf{M}(t))\rangle \approx N_1 \langle(\mathbf{D}_a(0), \mathbf{D}_a(t))\rangle \tag{3}$$

where $\mathbf{D}_a = \sum_\alpha \mathbf{d}_{a\alpha}$ is the dipole moment induced in the isolated solute a surrounded by solvent particles and the outer angular brackets denote statistical averaging. When $x = N_1/(N_1 + N)$ is increased, another solute b can intrude the first coordination sphere around a. As a result, two additional polarizations appear: first, $\mathbf{m}_{ab}$ is induced and, second, $\mathbf{D}_a$ is converted into $\mathbf{D}'_a$ where the prime means that a solvent particle in the nearest surrounding of a is substituted by the solute b. In other words, $\mathbf{D}'_a$ is the sum of $\mathbf{d}_{a\alpha}$ over the nearest solvent particles α, one of which is now missing. Thus, at small x the TACF (3) should be supplemented by a term quadratic in N_1

$$N_1^2 \langle(\mathbf{m}_{ab}(0) + \mathbf{D}'_a(0), \mathbf{m}_{ab}(t) + \mathbf{D}'_a(t))\rangle \tag{4}$$

Next, the term $\mathbf{d}'_{ab}$, which is in-phase with $\mathbf{m}_{ab}$, is to be separated from $\mathbf{D}'_a$: $\mathbf{d}'_{ab} \equiv \frac{\langle(\mathbf{D}'_a,\mathbf{m}_{ab})\rangle}{\langle(\mathbf{m}_{ab},\mathbf{m}_{ab})\rangle}\mathbf{m}_{ab} \equiv S_2\mathbf{m}_{ab}$ which leads to the "screened" binary polarization $\mathbf{m}'_{ab}$: $\mathbf{m}'_{ab} = \mathbf{m}_{ab} + \mathbf{d}'_{ab}$. Because of the screening, the total intensity of the $r-$line equals $\langle(\mathbf{m}'_{ab}, \mathbf{m}'_{ab})\rangle = (1+S_2)^2 \langle(\mathbf{m}_{ab}, \mathbf{m}_{ab})\rangle$. The remaining out-of-phase component of $\mathbf{D}'_a$ refers to the collective dynamics and contributes to the diffuse spectrum. Its interference with the in-phase component will be disregarded, for this effect does not change the integrated intensities and only slightly redistributes the intensity near the r-line.

Equations (2)-(4) can be used to qualitatively interpret the background integrated intensity ($M_b^{(0)}(x)$) behavior on going from LN_2 to LAr discussed in the previous section. We first notice that the linear terms dominating in highly diluted systems are very close to each other. This result seems to be unexpected from the conventional electrostatic induction model, for the used solvents have quite different properties, namely, N_2 posesses a quadrupole moment Q_{N_2} while all multipoles of Ar are vanishing. As a result, the N_2-O_2 interaction is characterized by two leading long-range induction channels, (I) the first due to the polarization of N_2 by the quadrupolar field of O_2 with the characteristic amplitude $Q'_{O_2}\hat{\alpha}_{N_2}$ and the other (II) for which the roles of solute and solvent are interchanged so that the relevant amplitude is $Q_{N_2}\hat{\alpha}'_{O_2}$. Here, $\hat{\alpha}_X$ denotes the molecular polarizability tensor (X =O_2, N_2) and the primed quantities are the derivatives with respect to the O_2 bond length. Since the channels are weakly interfering, $M_b^{(0)}$ is proportional to the sum of the squared amplitudes. Evidently, in the O_2-Ar case, channel II is missing that would be expected to reduce the intensity on going from LN_2 to LAr. In reality, however, the direct induction amplitude (I), as the data collected in Ref.[24] show, is three times larger than the amplitude II and, therefore, the channel II extinction in LAr decreases the intensity just by about 10 %. Besides, such attenuation of the background intensity can be compensated by its enhancement caused by a noticeable increase of the solvent number density ρ (cf. ρ_{N_2} = 597 Amagat and ρ_{Ar} =771 Amagat[25]).

In contrast to the linear-term invariance, the quadratic coefficient shows up a threefold increase on going from argon to nitrogen (Section III B). This seems to be hardly explicable without the notion of screening, for we are to consider the same O_2-O_2 interactions but occurring in the bulk of different solvents. Noteworthy, the mean polarizabilities of O_2, N_2 and Ar are close to each other (cf. 10.9, 11.7 and 11.1 a.u., respectively) and, hence, the (negative) screening is expectedly very strong. In a simplified picture,[16] the

screening coefficients scale as $(1-\alpha_X/\alpha_{O_2})^2$ where α_X is the solvent polarizability. Despite its crudeness, the model predicts a background intensity attenuation on going from N_2 to Ar, in compliance with our data.

Essentially, the r-line formation, its screening and a concomitant drastic slow down of the solute-solute diffusion are consequences of the many-body dynamics. In a gas under the regime of binary collisions, the screening is evidently abscent, $\mathbf{m}'_{ab} = \mathbf{m}_{ab}$, and the TACF (3) reduces to $N_1 N\langle(\mathbf{d}_{a\alpha}(0), \mathbf{d}_{a\alpha}(t))\rangle$. In concert with the self term $N_1^2\langle(\mathbf{m}_{ab}(0), \mathbf{m}_{ab}(t))\rangle$, it produces a diffuse spectrum, provided the contributions from the bound solute-solute ab and solute-solvent $a\alpha$ dimers are negligable. It should be noted that the bound spectra, even though they can be observed at low or moderate pressures, rapidly lose their line structure as the pressure is elevated (because of the reduction of the bound-state lifetimes) and become indistinguishable from the diffuse background formed by transitions in the continuous spectrum. Thus, if one applies the gas-like motion picture to a liquid, only the diffuse part of the spectrum can be rationalized.

Actually, it is the fast and chaotic variations of molecular velocity in a liquid that effectively retard the translations which, in addition, are strongly confined to the nearest surrounding. Altogether, this results in a profound slow down of the diffusion rate. In turn, the retardation manifests itself in a striking narrowing of the spectrum of $\mathbf{m}'_{ab}$ which is a function of the translational coordinate. Theoretically, this is a particular case of the motional narrowing (MN) of the spectrum of a certain physical quantity, depending on the generalized coordinate q, under the conditions of the fast relaxation rate of the velocity $\dot{q}$.[26] From the pressure narrowing of the NMR signals[27] and the Dicke effect[28] on, many other spectroscopic MN patterns produced by collisional rate enhancement have been discussed in the literature.[5,29–31]

However, in the allowed spectra the translational coordinates are not coupled to the electromagnetic field and thus remain silent. On contrary, they become spectroscopically active in CIA, which opens new vistas to directly trace transformations of the translational motion by density. Most strikingly, these transformations affect the solute-solute spectrum (4) solely determined by the dynamics of the single variable $\mathbf{R}_{ab}(\equiv \mathbf{R})$, the intermolecular separation vector. Its motion metamorphoses from rapid unbound translations in a gas into slow diffusion in the liquid phase. As a consequence, a resonance, quasi-Lorentzian $r-$line[15,16] emerges, more than one decimal order sharper than the gas-phase signature.

Contrastingly, the density narrowing of the quadrupole-induced hydrogen lines caused by the collective polarization (3), as studies[32,33] have shown, is much weaker and only halves the line widths. Diffusion thus rather indirectly shows itself up in such narrowing. Because of this, a semiempirical theory[34] operating with the conventional diffusion rate could only qualitatively explain the density narrowing[32,33] and failed to rationalize the newer experimental data.[35]

In the foregoing, the arguments presented suggest that the solute-solute r-line should disappear in a pure liquid. However, when a small amount of argon was dissolved in nitrogen, the r-line emerged. Because of the $x_{N_2}x_{Ar}$ scaling, it was ascribed to the N_2-Ar complexes.[6] Here, the effect is rationalized in a different way. First, the intrusion of an Ar atom (α) into the first coordination sphere around a vibrating N_2 molecule (a) induces a binary polarization ($\mathbf{d}_{a\alpha}$). Second, as the vibrations of different N_2 molecules are practically uncorrelated, it suffices to consider the action of a particular nitrogen molecule (a) on the Ar atom and then to multiply the resulting intensity by $N_{N_2}(= N_1)$. In other words, we are again dealing with the case of the binary polarization $\mathbf{d}_{a\alpha}$ dependent on a single translational coordinate $\mathbf{R}_{a\alpha}$ whose spectrum is motionally narrowed inasmuch as the one associated with the solute-solute interaction in a diluted solution was. When x_{Ar} is small, the interference between $\mathbf{d}_{a\alpha}$ and $\mathbf{d}_{a\beta}$ ($\beta \neq \alpha$) is negligible and therefore the solute-solvent induced r-line should scale as $N_1N \sim xx_{Ar}$, in an accord with the experimental results.[6] Since the nearest surrounding of the spectroscopically active N_2 molecule is perturbed by an Ar intruder, the solute-solvent r-line should be screened. Again, as x_{Ar} grows, the xx_{Ar} scaling of the r-line will be increasingly cancelled by the negative correlations between $\mathbf{d}_{a\alpha}$ and $\mathbf{d}_{a\beta}$ which might also broaden the line. Finally, when N_2 is isolated in the bulk of liquid Ar, these correlations completely wash out the resonance solute-solvent feature. Both mechanisms, *viz* the N_2-N_2 induction in the argon surrounding and the N_2-Ar induction in the N_2 surrounding, must be considered on equal footing and, when taken altogether, result in the maximal resonance intensity in an approximately equimolar mixture, in agreement with the experiment.[6]

2. Diffusional narrowing

Consider the behavior of the solute-solute part $\mathbf{m}(= \sum_{ab} \mathbf{m}_{ab})$ of the induced polarization (2). Neglecting the minute correlations between vibrational transitions in different solutes, it suffices to study the behavior of the screened polarization $\mathbf{m}'_a = \sum_b \mathbf{m}'_{ab}$ induced on a

certain spectroscopically active solute a by its interactions with other solutes. In doing so, we also assume $\mathbf{m}'_{ab}$ to be a function of $\mathbf{R}_{ab}$ only and not subjected to molecular rotations. The memory-function expression[26] for the spectral function $J_r(\Delta\omega)$ of $\mathbf{m}'_a$ reads:

$$J_r(\Delta\omega) = \frac{N_1\langle(\mathbf{m}'_a, \mathbf{m}'_a)\rangle}{\pi} \operatorname{Re} \frac{1}{i\Delta\omega + \Gamma_r(\Delta\omega)} \tag{5}$$

where $\Delta\omega$ is the detuning from the vibrational frequency ω_0. Denoting the projector on $\mathbf{m}_a$ by $\hat{P}_a$, the memory function in the classical limit can be written as

$$\Gamma_r(\Delta\omega) = \frac{1}{N_1\langle(\mathbf{m}_a, \mathbf{m}_a)\rangle} \times \int_0^\infty e^{-i\Delta\omega t}\langle\sum_b(\nabla\mathbf{m}_{ab}, \mathbf{v}_{ab})|e^{iQ_aLQ_at}|\sum_c(\nabla\mathbf{m}_{ac}, \mathbf{v}_{ac})\rangle dt \tag{6}$$

where $\hat{Q}_a = 1 - \hat{P}_a$, $\mathbf{v}_{ik} = \mathbf{v}_i - \mathbf{v}_k$ is the relative velocity of the solute $i-k$ pair and $\hat{L}$ is the Liouvillian of the translational motion. In the MN regime, the velocities decorrelate (with the typical rate $t_v'^{-1}$) much faster than $\nabla\mathbf{m}_{ab}$ and $\nabla\mathbf{m}_{ac}$ which can be thus considered as time-independent quantities. In the frequency range $\Delta\omega \ll t_v'^{-1}$, $\Gamma_r(\Delta\omega) \approx \Gamma_r(0) \sim t'_v$ holds wheareas $J_r(\Delta\omega)$ (5) reduces into a Lorentzian. Besides, the solute-solvent interactions at small or moderate x dominate over the solute-solute ones that renders the velocities of different solute molecules uncorrelated to one another. To further simplify the calculation, assume also that the configuration and velocity averagings can be performed independently. The result

$$\Gamma_r(0) = m_2 t'_v \tag{7}$$

is thus expressed via the reduced second-order moment m_2 of the $\mathbf{m}_a$ spectrum and the solute velocity decorrelation time $t'_v = (\mu/3kT)\int_0^\infty\langle(\mathbf{v}_a|e^{iQ_aLQ_at}|\mathbf{v}_a)\rangle dt$ where μ stands for the solute mass. Notice that, even under the above simplifying assumptions, t'_v still differs from the conventional velocity decorrelation time t_v which defines the macroscopic diffusion rate and whose definition does not contain the projector $\hat{Q}_a$.[26] In other words, t'_v derived from the CIA spectra is a microscopic-scale characteristics which cannot be directly used to determine the macroscopic diffusion rate.

It should be stressed that the factorization (7) of $\Gamma_r(0)$ into the static (m_2) and dynamic (t'_v) quantities bears a semiquantitative character whose accuracy needs further verification and was done primarily to facilitate the further analysis. When the solute-solute and solute-solvent interaction potentials differ little, t'_v is weakly subjected to x and the $\Gamma_r(0)$ vs x

behavior is almost entirely determined by the static quantity m_2

$$m_2 \equiv \frac{2kT}{\mu} \frac{\langle(\nabla \mathbf{m}_{ab}, \nabla \mathbf{m}_{ab}) + N_1(\nabla \mathbf{m}_{ab}, \nabla \mathbf{m}_{ac})\rangle}{\langle(\mathbf{m}_{ab}, \mathbf{m}_{ab}) + 2N_1(\mathbf{m}_{ab}, \mathbf{m}_{ac})\rangle} \tag{8}$$

which is much simpler for the analysis. The denominator in (8) can be written as

$$\langle(\mathbf{m}_{ab}, \mathbf{m}_{ab}) + 2N_1(\mathbf{m}_{ab}, \mathbf{m}_{ac})\rangle = \langle m_{ab}m_{ab} + 2N_1 m_{ab}m_{ac}z_{abc}\rangle$$

where z_{abc} is the cosine of the angle between $\mathbf{R}_{ab}$ and $\mathbf{R}_{ac}$ and $m_{ik}(R_{ik})$ is the projection of $\mathbf{m}_{ik}$ onto $\mathbf{R}_{ik}$. The interference between the induced dipoles $\mathbf{m}_{ab}$ and $\mathbf{m}_{ac}$ is typically negative[23] and tends to cancel the positive definite binary self term $\langle(\mathbf{m}_{ab}, \mathbf{m}_{ab})\rangle$. Such cancellation effect[23] strongly manifests itself in dense media in which the relative translations transform into quasioscillations for which $z_{abc} \approx -1$ holds. As the result, in a dense fluid (i.e. at $x \to 1$) the cross term can compensate about three quarters of the self term.

To analyze the concentration behavior of the numerator in (8), the nabla operator and the dipole moments were treated as irreducible spherical tensors (IST) of rank one. By applying the IST techniques (see Appendix), we obtained

$$\langle(\nabla \mathbf{m}_{ab}, \nabla \mathbf{m}_{ac})\rangle = \langle[g_{0ab}g_{0ac} + 2g_{2ab}g_{2ac}P_2(z_{abc})]\rangle/3 \tag{9}$$

where $g_{0ik} = dm_{ik}/dR_{ik} + 2m_{ik}/R_{ik}$, $g_{2ik} = dm_{ik}/dR_{ik} - m_{ik}/R_{ik}$ and P_2 is the second-degree Legendre polynomial. Equation (9) can also apply for the self term, if we set $b = c$ and $P_2(1) = 1$. In doing so, the second-order moment expression derived for the translational absorption induced by binary collisions between spherically symmetric particles is reproduced.[36] Since in a condensed medium the amplitudes of the solute translations are much smaller than the mean intermolecular separations, the most probable configurations correspond to $R_{ab} \approx R_{ac}$ so that the products $g_{Nab}g_{Nac}$ (N=0,2) are, in the mean, positive. As $P_2(z_{abc}) \approx P_2(-1) = 1$, the gradient interference term is expectedly positive. It should be therefore anticipated that, as x grows, the numerator of (8) is increased whereas the denominator is decreased. In other words, a substantial concentration broadening of the r-line is expected that is accompanied by a retardation of its intensity growth. On going to the pure liquid, both trends can finally make the r-line indistinguishable from the broader pedestal absorption. Besides, it should be kept in mind that the validity of Eq. (7) relies on the assumption of slow translational relaxation, or $\Gamma_r t'_v = m_2 t'^2_v \ll 1$. At high x, the concentration broadening can render $\Gamma t'_v$ comparable to unity that, in turn, could manifest itself in the nonLorentzian solute-solute line shape.

In the studied concentration range, some of these predictions are conspicuous. First, the r-line growth retardation for the O_2-LAr system can be seen from Fig. 5 at $x \gtrsim 0.1$. To make the effect more contrast, the intensity of the r-line relative to the total band moment $M_t^{(0)}$ is plotted on Fig. 6. Notice that the behavior of $M_t^{(0)}(x)$ is almost linear in the whole concentration range studied. As demonstrated by Fig. 6, the ratio $M_r^{(0)}/M_t^{(0)}$ also varies linearly at small x ($x \leq 0.07$) suggesting $M_r^{(0)}(x)$ to scale as x^2. Outside that range, the growth of $M_r^{(0)}/M_t^{(0)}$ is increasingly saturated betoking that $M_r^{(0)}(x) \sim x$ and thus strongly deviates from the initial quadratic scaling. Such linear $r-$line scaling detected at the fundamental N_2 frequency in the N_2-LAr cryosystem[6] at $x_{N_2} \geq 0.1$ was used as an argument in favor of the N_2-Ar complex formation. The present study, though confirming the linear scaling law at moderate x, proves the r-line to originate at high dilutions rather from the solute-solute "complexes" but not from the "solute-solvent" ones. Furthermore, these complexes are formed, as the MN theory shows, not because of the local potential well but merely because two solute molecules are blocked in a cage formed by the surrounding solvents.

Another experimental fact to be rationalized is a substantial decrease[6] of $M_r^{(0)}$ with growing temperature; for instance, $M_r^{(0)}$ of the N_2-Ar solution with x_{N_2}=0.8 was approximately halved when the temperature was raised from 82 up to 117 K. The effect was interpreted[6] by the thermal depletion of the solute-solvent complexes. Apart from the criticism of the complexation hypothesis set out in Introduction, it should be mentioned that such temperature rise is accompanied by a substantial (about 22 %) density decrease to which the CIA spectra are especially sensitive. Based on the fact that the mean intermolecular separation $\bar{R}$ scales as $\rho^{-1/3}$, a rough estimation of the density effect can be easily performed. For that, we adopt the dispersion model[37] of the longest-range isotropic solute-solvent dipole moment $\mathbf{d}$ which fades away as R^{-7}. Since $M_r^{(0)}$ correlates with $d^2(\bar{R})$, the density decrease dampens the intensity by a factor of $1.22^{-14/3} \approx 0.43$ that favorably corresponds to the measured attenuation. Hence, to interpret the $r-$line temperature behavior, one does not need to resort to the notion of energetically stable complexes.

A similar picture of the solute-solvent r-line vs x behavior is expected in the O_2-LAr system, for the properties of molecular oxygen are akin to those of N_2. To restore a fuller picture, spectral measurements should be extended to larger values of x paying special attention to the r-line evolution in the LO_2 solutions with small content of argon.

However, we were unable to detect the concentration broadening of the r-line. Instead, as x was increased up to 0.23, the line appeared to be slightly narrowed (by 20%) in both cryosolutions. The effect is hardly explicable if one applies the factorization aproximation and then accounts solely for the static factor (8). In the O_2-LAr case, the ternary contributions to $M_r^{(0)}$ are negative and cancel the binary term by $\sim$40 % at x=0.23. Therefore, to obtain the 20 % decrease of Γ_r, the numerator of (8) should decrease by $\sim$50 %, hardly believable from the aforementioned arguments. Except the crudeness of the factorization approximation and the so far neglected concentration dependence of t'_v, there are other effects which might compete with the translational MN and thus affect the Γ_r vs x behavior. First, it is the residual motionally-narrowed vibration-rotation splitting[5,30] and, second, the vibrational dephasing.[5,30] In order to appreciate the relative importance of the processes involved, IR studies are desirable in broader concentration and density ranges as well as in the overtone bands.

IV. SYNOPSIS

New data on the collision-induced spectra of molecular oxygen dissolved in the liquids argon and nitrogen (T=89 K) are reported with special emphasis made on the paradoxically sharp feature, the r-line, developing at the fundamental vibrational frequency ($\tilde{\nu}_0[O_2]$ =1556 cm^{-1}). In line with our previous findings for the similar feature in the pH$_2$-LNe spectra,[15,16] this investigation proves the r-line in diluted solutions ($x \lesssim 0.07$) to scale quadratically with the oxygen mole fraction x. This result implies the resonance feature to originate from the solute-solute (O_2-O_2) interactions. As the O_2 rotation in inert solutions generates a broad spectrum, the r-line should be entirely assigned to the isotropic part of the induced dipole moment which does not depend on the O_2 axis orientation. The Lorentzian r-line shape with HWHH as low as one cm^{-1}) pinpoints the motional narrowing (MN) of the O_2-O_2 translational spectrum. In turn, MN is directly related to the microscopic-scale diffusion in liquids, a fundamental process remained up to now inaccessible to spectroscopic means. The newly found spectral features thus open up new vistas for studies of translational microdynamics of the reference simple liquids.

ACKNOWLEDGMENTS

Financial support from the Special Research Fund of the University of Antwerp, the FWO-Vlaanderen and from the Special Research Fund of the Saint-Petersburg State University (Project No. 11.38.265.2014) is gratefully acknowledged.

APPENDIX

For generality, we shall consider the action of the gradient operator $\nabla(= \nabla^{(1)})$[38]

$$\nabla^{(1)} = C^{(1)}(\Omega)\frac{\partial}{\partial R} + \frac{1}{R}\nabla^{(1)}_{\Omega} \tag{10}$$

on an arbitrary IST $D^{(l)} = d(R)C^{(l)}(\Omega)$ depending on the separation $\mathbf{R} = (R, \Omega)$ between two spherical particles; for brevity, we drop hereafter the molecular labels and the labels of spherical tensor components. For convenience, the Racah harmonics[38] $C^{(l)}_m$ shall be mostly exploited instead of the conventional spherical harmonics $Y^{(l)}_m$. The results thus derived might be useful for many cases of importance to the collision-induced spectroscopies, e.g. the (isotropic) dipole moment $\mathbf{m} = m^{(1)} \equiv m(R)C^{(1)}(\Omega)$, the induced anisotropic polarizability, etc. The nabla operator transforms $D^{(l)}$ into a linear combination of ISTs $C^{(l')}(\Omega)$:

$$\nabla^{(1)}D^{(l)} = \sum_{l'}\{\nabla^{(1)} \otimes d(R)C^{(l)}(\Omega)\}^{(l')} \equiv \sum_{l'} g_{l'}(R)C^{(l')}(\Omega) \tag{11}$$

where $\{. \otimes .\}^{(l')}$ designates the contraction of two ISTs into an IST of rank l'. The action of the radial part of $\nabla^{(1)}$ on $D^{(l)}$ is simple

$$\frac{\partial d(R)}{\partial R}\{C^{(1)} \otimes C^{(l)}\}^{(l')} = \frac{\partial m(R)}{\partial R}C^{l'0}_{l010}C^{(l)}(\Omega) \tag{12}$$

where $C^{l'0}_{l010}$ are the Clebsch-Gordan coefficients distinct from zero only at $l' = l \pm 1$: $C^{l'0}_{l010} = \sqrt{\frac{l+1}{2l+1}}\delta_{l'l+1} - \sqrt{\frac{l}{2l+1}}\delta_{l'l-1}$. To derive the angular term, one should expand it in spherical harmonics and apply the Wigner-Eckart theorem[38]

$$\begin{aligned}\nabla^{(1)}_{\Omega\rho}C^{(l)}_{\sigma}(\Omega) &= \sqrt{\frac{4\pi}{2l+1}}\nabla^{(1)}_{\Omega\rho}Y^{(l)}_{\sigma}(\Omega) = \sqrt{\frac{4\pi}{2l+1}}\sum_{l'm'} Y^{(l')}_{m'}\langle Y^{(l')}_{m'}|\nabla^{(1)}_{\Omega\rho}|Y^{(l)}_{\sigma}\rangle \\ &= \frac{1}{\sqrt{2l+1}}\sum_{l'm'} C^{(l')}_{m'}(\Omega)C^{l'm'}_{1\rho l\sigma}\langle l'||\nabla^{(1)}_{\Omega}||1\rangle\end{aligned} \tag{13}$$

where $\langle l'||\nabla_\Omega^{(1)}||l\rangle = -[l\sqrt{l+1}\delta_{l'l+1} + (l+1)\sqrt{l}\delta_{l'l-1}]$ is the reduced matrix element of $\nabla_\Omega^{(1)}$.[38] The tensor (13) has the irreducible components

$$\sum_{l'm'\rho\sigma} C_{1\rho l\sigma}^{l'm} \nabla_{\Omega\rho}^{(1)} C_\sigma^{(l)}(\Omega) = \frac{1}{\sqrt{2l+1}} \sum_{l'} C_m^{(l')}(\Omega) \langle l'||\nabla_\Omega^{(1)}||l\rangle \tag{14}$$

with the ranks $l' = l \pm 1$. Taken together, the angular and radial contributions produce the following nonvanishing coefficients in Eq. (11)

$$g_{l-1}(R) = -\sqrt{\frac{l}{2l+1}}[\frac{dd}{dR} + (l+1)\frac{d}{R}];\ g_{l+1}(R) = \sqrt{\frac{l+1}{2l+1}}[\frac{dd}{dR} - l\frac{d}{R}] \tag{15}$$

Next, we adopt the factorization approximation for the velocity and configuration averagings. For either of the two statistical procedures, only scalar contractions of ISTs of the same rank survive because of the macroscopic isotropy. Accounting for this fact and using the addition theorem,[38] a compact general expression for the ternary term is easily derived

$$\langle(\nabla D_{ab}^{(l)}, \nabla D_{ac}^{(l)})\rangle = \langle g_{l-1}(R_{ab}) g_{l-1}(R_{ac}) P_{l-1}(z_{abc}) + g_{l+1}(R_{ab}) g_{l+1}(R_{ac}) P_{l+1}(z_{abc})\rangle \tag{16}$$

Barocchi et al result[39] for the dipole-induced dipole (DID) polarizability, $\beta_{DID}^{(2)} \sim R^{-3} C^{(2)}(\Omega)$, immediately follows from (16) as a particular case. Remarkably, for any harmonic interaction-induced IST $D^{(l)}$ (i.e. one behaving as $R^{-l-1}C^{(l)}(\Omega)$), the g_{l-1} coefficient is annuled and the first term of (16) dissappears. This result obviously applies for $\beta_{DID}^{(2)}$ as well as for a practically important case of the multipole-induced dipole moments.[2,3]

The binary term ($b = c$) of the second-order moment is straightforwardly derived from (16) by setting $z_{abc} = 1 = P_{l-1}(1) = P_{l+1}(1)$ so that the resultant expression reduces to a sum of squares, $\langle(dd_{ab}/dR_{ab})^2 + l(l+1)(d_{ab}/R_{ab})^2\rangle$, which respectively represent particular contributions from the radial and angular degrees of freedom. By contrast, the mixed products of the $d-$functions and its derivatives always show up in the ternary term (16).

REFERENCES

[1]M.F. Crawford, H.L. Welsh, and J.L. Locke, Phys. Rev. **75**, 1607 (1949).

[2]J. Van Kranendonk, Physica **73,** 156 (1974).

[3]L. Frommhold, *Collision-Induced Absorption in Gases* (Cambridge Uinversity Press, Cambridge, 1993).

[4]A.P. Kouzov, in: *Molecular Cryospectroscopy*, Advances in Spectroscopy, Vol. 23, edited by R.J.H. Clark and R.E. Hester (Wiley & Sons, Chichester, 1995), Chap. 6.

[5]J.-M. Hartmann, C. Boulet, and D. Robert, *Collisional Effects on Molecular Spectra* (Elsevier, Amsterdam, 2008).

[6]W.A. Herrebout, A.A. Stolov, E.J. Sluyts, and B.J. van der Veken, Chem. Phys. Lett. **295,** 223 (1998).

[7]R.D. Beck, M.F. Hineman, and J.W. Nibler, J. Chem. Phys. **92**, 7068 (1990).

[8]De T. Sheng and G.E. Ewing, J. Chem. Phys. **55**, 5425 (1971).

[9]D.R. Bosomworth and H.P. Gush, Can. J. Phys. **43**, 751 (1965).

[10]U. Buontempo, S. Cunsolo, G. Jacucci, and J.J. Weis, J. Chem. Phys. **63**, 2570 (1975).

[11]A.S. Davydov, *Quantum Mechanics* (Pergamon Press, Oxford, 1965).

[12]S. Flügge, *Practical Quantum Mechanics I* (Springer, Berlin, 1971).

[13]J.E. Lennard-Jones and A.F. Devonshire, Proc. R. Soc. Lond. A **63**, 53 (1937).

[14]M.O. Bulanin, M.G. Melnik, and M.V. Tonkov, Opt. Spektrosk. **23**, 714 (1967).

[15]W.A. Herrebout, B.J. van der Veken, and A.P. Kouzov, Phys. Rev. Lett. **101**, 093001 (2008).

[16]W.A. Herrebout, B.J. van der Veken, and A.P. Kouzov, J. Chem. Phys. **137**, 084509 (2012).

[17]W.H. Fletcher and J.S. Raydide, J. Raman Spectr. **2**, 3 (1974).

[18]The band center-of-mass frequency is provided to which an isotropic Raman band collapses in the motional narrowing regime.[5,30]

[19]H. Kiefte, M.J. Clouter, N.H. Rich and S.F. Ahmad, Chem. Phys. Lett. **70,** 425 (1980).

[20]J. Kreutz and H.J. Jodl, Phys. Rev. B **68**, 214303 (2003).

[21]A.P. Kouzov, Opt. Spectrosk. **30**, 841 (1971).

[22]Hereafter, the digits in parenthesis are uncertainties in units of the last signicant digits.

[23]J. Van Kranendonk, Physica **23**, 825 (1957).

[24]G. Moreau, J. Boissole, R. Le Doucen, C. Boulet, R.H. Tipping, and Q.Ma, J.Q.S.R.T. **69,** 245 (2001).

[25]N.B. Vargaftik, *Tables on the Thermophysical Properties of Liquids and Gases* (Halsted Press, New York, 1975).

[26]D. Forster, *Hydrodynamic Fluctuations, Broken Symmetry and Correlation Functions* (Benjamin, Reading, MA, 1975).

[27]A. Abragam, *Principles of Nuclear Magnetism* (International Series of Monographs on Physics) Oxford University Press, Oxford, 1983)

[28]R.H. Dicke, Phys. Rev. **89**, 472 (1953).

[29]G.V. Mikhailov, Lebedev Physical Institute Trans. (in Russian) **27,** 150 (1964).

[30]A.I. Burshtein and S.I. Temkin, *Spectroscopy of Molecular Rotation in Gases and Liquids* (Cambridge University Press, Cambridge, 1994)

[31]N.N. Filippov and M.V. Tonkov, J. Chem. Phys.**108**, 3608 (1998).

[32]J. De Remigis, J.W. MacTaggart, and H.L. Welsh, Can. J. Phys. **49**, 381 (1971).

[33]J.W. MacTaggart, J. De Remigis, and H.L. Welsh, Can. J. Phys. **51**, 1971 (1973).

[34]H.R. Zaidi and J. Van Kranendonk, Can. J. Phys. **49**, 385 (1971).

[35]U. Buontempo, S. Cunsolo, P. Dore, and P. Maselli, Mol. Phys. **37**, 779 (1979).

[36]J.D. Poll and J.L. Hunt, Can. J. Phys. **54**, 461 (1976).

[37]J.E. Bohr and K.L.C. Hunt, J. Chem. Phys. **86**, 5441 (1987).

[38]D.A. Varshalovich, A.N. Moskalev, and V.K. Khersonskii, *Quantum Theory of Angular Momentum* (World Scientific, Singapore, 1988).

[39]F. Barocchi, M. Neri, and M. Zoppi, Mol. Phys. **34**, 1391 (1977).